Indexed in Medline!

ROYAL SOCIETY
OF CHEMISTRY

PAPER
Takuma Ohtawa and Makoto Tsunoda
An on-line heart-cutting two-dimensional liquid
chromatography method for intracellular 2-hydroxyglutarate
enantiomers

PAPER

Check for updates

An on-line heart-cutting two-dimensional liquid chromatography method for intracellular 2-hydroxyglutarate enantiomers

Takuma Ohtawa and Makoto Tsunoda [ID] *

D-2-Hydroxyglutarate (D-2-HG) is an oncometabolite that induces cancer cell survival and growth. D-2-HG is produced by mutations in isocitrate dehydrogenases 1 and 2. L-2-HG has different roles than the D-form, and chiral discrimination is important for elucidating the exact roles of the 2-HG enantiomers. In this study, an analytical method for 2-HG enantiomers was developed using on-line heart-cutting two-dimensional liquid chromatography (2D-LC) with fluorescence detection. Fluorescence derivatization of 2-HG with 4-nitro-7-piperazino-2,1,3-benzoxadiazole (NBD-PZ) was performed using 4-(4,6-dimethoxy-1,3,5-triazin-2-yl)-4-methylmorpholinium chloride, a hydrophilic condensing reagent, at 70 °C for 30 min. The first dimension on the octadecylsilyl column was aimed at separating NBD-PZ-2-HG from other compounds obtained *via* derivatization or from biological fluids. The NBD-PZ-2-HG peak was fractionated into a sample loop and automatically injected into the second dimension. In the second dimension, a CHIRALPAK IC column separated NBD-PZ-D- and L-2-HG with a resolution of 2.14. The limits of quantification were 0.25 pmol per injection for NBD-PZ-D-2-HG and-L-2-HG. The precision values were below 6.58%, and the accuracies were 88.2–92.8%. The intracellular concentrations of D-2-HG and L-2-HG in the cancer cells were 13.5 ± 0.4 and 9.9 ± 0.3 pmol per 1.0×10^6 cells, respectively. The developed method will be useful for elucidating the role of 2-HG enantiomers in cancer cells.

Introduction

Metabolic reprogramming is a phenomenon in which cells change their metabolic pathways in response to stimuli from the surrounding environment. Cancer cells often undergo specific metabolic reprogramming by mutated metabolic enzymes, and the concentrations of cellular-specific metabolites change.[1–3] These compounds are called oncometabolites, and they promote cancer growth and survival. 2-Hydroxyglutarate (2-HG) is an oncometabolite that has enantiomers. Generally, D-2-HG is generated from α-ketoglutarate (α-KG) by hydroxyacid-oxoacid transhydrogenase, whereas L-2-HG is generated from α-KG by L-malate dehydrogenase. However, both D- and L-2-HG are converted to α-KG by D- and L-2-HG dehydrogenases, respectively. These conversions contribute to the lowering of the 2-HG concentration in cells.[4–6] The oncometabolite 2-HG is associated with the mutation of isocitrate dehydrogenases 1 and 2 (IDH1/2). Wild-type IDH1/2 metabolizes isocitrate to α-KG and protects the cells from oxidative stress. IDH1/2 mutations, which are observed in gliomas, acute myeloid leukemia, and other malignancies, lose their normal ability and produce D-2-HG from α-KG (Fig. 1). The rate of D-2-HG production exceeds that of elimination, and D-2-HG accumulates in cells.[7–13] In contrast, L-2-HG is not associated with IDH1/2 mutations but its production is reported to increase under hypoxic conditions.[14] Thus, enantiomeric separation of 2-HG is necessary to elucidate the roles of 2-HG enantiomers.

To date, several methods for analyzing 2-HG enantiomers have been developed. Gas chromatography and liquid chromatography (LC) are generally used to separate the 2-HG enantiomers, although most methods that use gas chromatography have not been fully validated.[15–17] Chiral derivatization, a chiral mobile phase, or a chiral stationary phase is used to separate the 2-HG enantiomers using LC. In the first approach, the 2-HG enantiomers are converted into diastereomers.[18,19] Diacetyl-L-tartaric anhydride[18] and *N*-(*p*-toluenesulfonyl)-L-phenylalanyl chloride[19] have been used as chiral derivatization reagents for 2-HG enantiomers. Both reagents have been successful in the baseline separation of derivatized 2-HG enantiomers and have been applied to biological samples.[18,19] However, chiral derivatization has several drawbacks. First, chiral derivatization reagents must be enantiomerically pure, which is difficult to achieve. Second, derivatization might cause racemization, although none of the developed methods have been tested in this regard. A chiral mobile phase method for 2-HG enantiomers was recently developed using copper(II) acetate and *N*,*N*-dimethyl-L-phenylalanine as chiral mobile phase

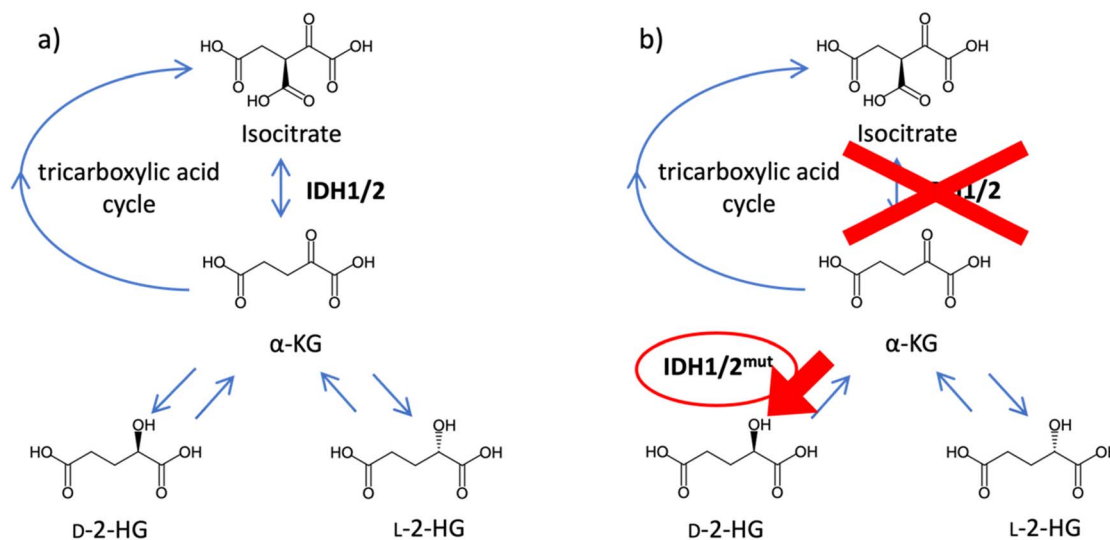*Graduate School of Pharmaceutical Sciences, University of Tokyo, Tokyo, Japan. E-mail: makotot@mol.f.u-tokyo.ac.jp*

Fig. 1 The relation between IDH1/2 and 2-HG. (a) Wild-type IDH1/2 and (b) mutant IDH1/2.

additives.[20] This method requires no derivatization, but suffers from a bad peak shape and low sensitivity.

In our previous study,[21] a heart-cutting two-dimensional liquid chromatography (2D-LC) system with fluorescence detection for intracellular 2-HG enantiomers was developed. An octadecylsilyl (ODS) column was used in the first dimension to separate 2-HG derivatized with 4-nitro-7-piperazino-2,1,3-benzoxadiazole (NBD-PZ) from other endogenous compounds, and a chiral column was used in the second dimension to separate the 2-HG enantiomers. This method succeeded in quantifying intracellular 2-HG enantiomers. However, fractionation in the first dimension was performed manually, which may have lowered the accuracy and precision and reduced the daily throughput. Accordingly, this study aimed to develop an on-line 2D-LC method for 2-HG enantiomers in biological samples and obtain better accuracy and precision.

Experimental

Chemicals

D-α-Hydroxyglutaric acid disodium salt and L-α-hydroxyglutaric acid disodium salt were purchased from Sigma-Aldrich (St. Louis, MO, USA). Hydroxyglutaric acid sodium salt was obtained from Cayman Chemical (Ann Arbor, MI, USA). NBD-PZ was obtained from Tokyo Chemical Industry (Tokyo, Japan). 4-(4,6-Dimethoxy-1,3,5-triazin-2-yl)-4-methylmorpholinium chloride n-hydrate (DMTMM) and trifluoroacetic acid (TFA) were purchased from FUJIFILM Wako Pure Chemical (Osaka, Japan). Formic acid was obtained from Kanto Chemical (Tokyo, Japan). Methanol and acetonitrile (HPLC grade) were purchased from Merck KGaA (Darmstadt, Germany). A Milli-Q system (Merck) was used for water purification.

Cell samples

U937, a human promonocytic leukemia cell line derived from a patient with histiocytic lymphoma, was obtained from the American Type Culture Collection (ATCC; Manassas, VA, USA), and cell line authentication testing was performed by the ATCC using a standardized short tandem repeat analysis. U937 cells were maintained in Roswell Park Memorial Institute 1640 medium containing 10% fetal bovine serum, 100 IU m^{-1} penicillin, and 100 μg mL^{-1} streptomycin. Prior to derivatization, the U937 cells were washed twice with phosphate-buffered saline, treated with 80% methanol, and centrifuged to remove insoluble particles. The supernatant was collected and dried via vacuum centrifugation. Dried cell samples (1×10^6 cells) were dissolved in 100 μL of water to prepare cell solutions.

Derivatization procedure

Standard or cell samples (50 μL) were mixed with 2 mmol L^{-1} NBD-PZ in acetonitrile (100 μL) and 280 mmol L^{-1} DMTMM in water (100 μL). The mixture was heated at 70 °C for 30 min. Subsequently, the solution was cooled on ice for 1 min, and 250 μL of 0.1% (v/v) TFA aqueous solution was added.

HPLC conditions

An on-line 2D-LC method was developed in this study. The LC system was composed of a PU-2080 pump, a LG-2080-02 ternary gradient unit, a DG-980-50 3-line degasser, an AS-950 autosampler, and an FP-2020 fluorescence detector for the first dimension; an HV-992-01 column selection unit, a PU-2080 pump, and an FP-2025 Plus fluorescence detector for the second dimension (Jasco, Tokyo, Japan); and a CO-631C column oven (GL Sciences, Tokyo, Japan) for both dimensions. The derivatized solution (5 μL) was injected into an Inertsil ODS-4 column (250 mm × 1.5 mm, 5.0 μm; GL Sciences) at 40 °C. The mobile phase was 0.05% (v/v) TFA in a water/acetonitrile (75/25, v/v) mixture and the flow rate was set to 0.075 mL min^{-1}. The eluate from 28.3 to 32.3 min of the first dimension was fractionated automatically and was injected into the second dimension, a CHIRALPAK IC column (150 mm × 4.6

mm, 5.0 µm; Daicel, Osaka, Japan). The mobile phase was a methanol/acetonitrile/formic acid aqueous solution (pH 2.0) (80/15/5, v/v/v), and the flow rate was 0.3 mL min^{-1}. The column was heated to 40 °C. Fluorescence detection was conducted at excitation and emission wavelengths of 491 and 547 nm, respectively.

Method validations

Linearity was calculated by analyzing standard samples of D- and L-2-HG (0.5–100 µM). Peak heights were plotted against their concentrations. The slopes, intercepts, and correlation coefficients of determination of the calibration curves were calculated using least-squares regression. The limits of quantification (LOQs) were calculated based on a signal-to-noise ratio of 10 using 0.5 µM D- and L-2-HG standards. Intra- and inter-day precisions were evaluated by measuring the same standard samples (lower LOQ: 0.5 µM, low: 5 µM, middle: 10 µM, high: 50 µM for both 2-HG enantiomers) four times in one day or on four different days, respectively. The precision and accuracy of the cells were evaluated using the U937 cells. The precision was calculated by measuring the same U937 sample four times, whereas the accuracy was evaluated by adding known concentrations of 2-HG standards to the cell sample (low: 5 µM, middle: 10 µM, high: 20 µM for both 2-HG enantiomers).

Results and discussion

Optimization of derivatization conditions

To decrease the influence of the mobile phase of the first dimension on the second dimension, the internal diameter of the ODS column was changed from 3.0 (used in our previous study) to 1.5 mm. However, an increase in column pressure was observed during the experiments, and the column eventually became clogged. This was attributed to the precipitation of triphenylphosphine, the hydrophobic compound used for derivatization. Therefore, DMTMM, which is soluble in water, was used as the condensation reagent instead of triphenylphosphine and 2,2′-dipyridyl-disulfide. The reaction using DMTMM, which has been previously reported, is described in Fig. 2.[21]

First, the effects of the organic solvents used in the derivatization reaction on the peak area of NBD-PZ-2-HG were investigated using methanol and acetonitrile. When acetonitrile was used, the peak area of NBD-PZ-2-HG was 2.5 times larger than when methanol was used. This may be because the carboxyl group of 2-HG forms a methyl ester with methanol and a condensing agent, and the reaction does not proceed well.
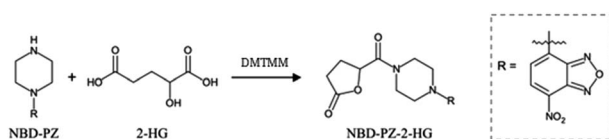

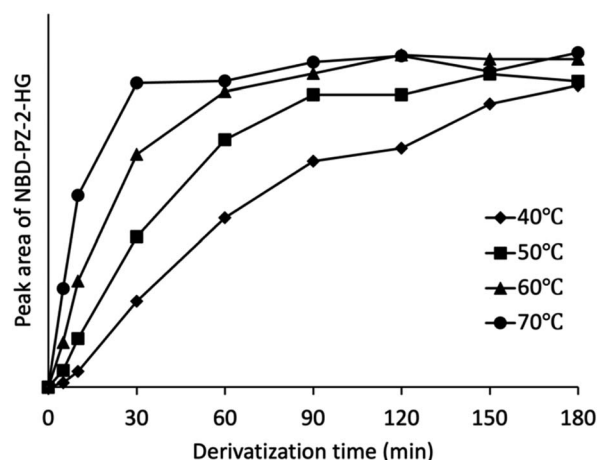Fig. 2   The reaction of NBD-PZ and 2-HG.

Fig. 3   Relationship between the derivatization time and peak area of NBD-PZ-2-HG.

Accordingly, acetonitrile was chosen as the solvent to dissolve NBD-PZ.

Next, the derivatization temperature and time were optimized. Fig. 3 shows the peak area as a function of derivatization time at temperatures of 40, 50, 60, and 70 °C. The derivatization proceeded faster with increasing temperature. Among the reactions that were deemed to have progressed sufficiently, the shortest derivatization time of 30 min and a temperature of 70 °C were chosen as the optimal temperature and time. Temperatures above 70 °C were considered inappropriate because the azeotropic point for the mixture of acetonitrile and water was 76 °C.

Optimization of separation conditions

The separation conditions in the first dimension were examined based on a previous study. The inner diameter of the column was reduced from 3.0 to 1.5 mm. Because the amount of mobile phase used is proportional to the square of the inner diameter of the column, halving the inner diameter reduces the amount of mobile phase used to 1/4. Therefore, when the retention time is the same, the mobile phase usage is expected to reduce to one quarter of the original. This reduces the influence of the mobile phase of the first dimension on the second dimension, resulting in a more stable analytical process. In addition, a reduction in the amount of mobile phase used is expected to reduce the analytical costs and environmental impact. The previously optimized mobile phase, water/acetonitrile/TFA (70/30/0.05, v/v/v), gave a resolution of 1.47 between a blank peak and the NBD-PZ-2-HG peak. Therefore, the mobile phase was changed to water/acetonitrile/TFA (75/25/0.05, v/v/v) and the polarity was increased to prolong retention, which improved the resolution to 2.29 and resulted in complete separation of NBD-PZ-2-HG from the blank peak.

Development of an on-line 2D-LC system

An on-line 2D-LC system was constructed, as shown in Fig. 4. Before injection, the system was operated in state A, which was
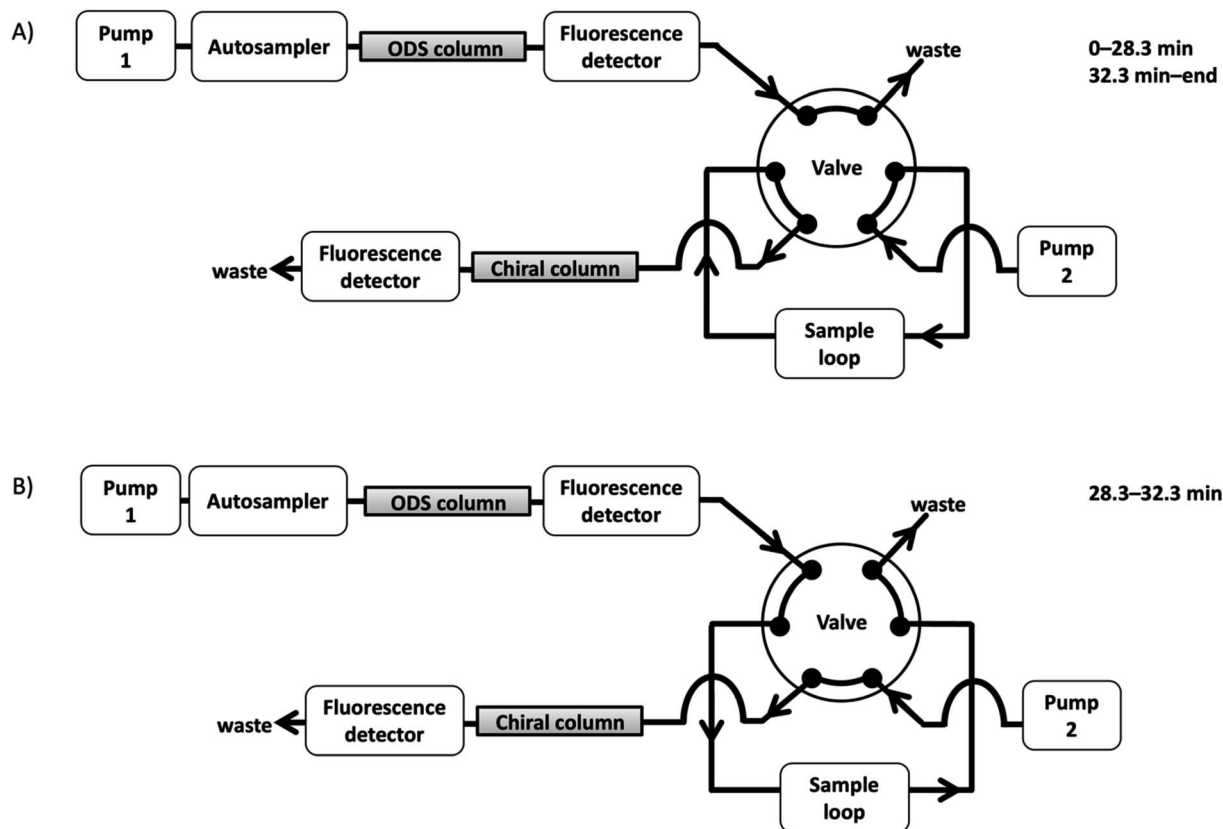
Fig. 4 On-line 2D-LC system. First dimension: the column was Inertsil ODS-4 column (250 mm × 1.5 mm, 5.0 μm), the mobile phase was 0.05% (v/v) TFA in water/acetonitrile (75/25, v/v), the flow rate was 0.075 mL min^{-1}, and the column temperature was 40 °C. Second dimension: the column was a CHIRALPAK IC column (150 mm × 4.6 mm, 5.0 μm), the mobile phase was a methanol/acetonitrile/formic acid aqueous solution (pH 2.0) (80/15/5, v/v/v), the flow rate was 0.3 mL min^{-1}, and the column temperature was 40 °C. Fluorescence detection was conducted at excitation and emission wavelengths of 491 and 547 nm, respectively. From injection to 28.3 min, the system was run in state A. Then, the valve was switched to state B and NBD-PZ-2-HG was loaded into the sample loop. After 32.3 min from the time of injection, the valve was switched back to state A, and NBD-PZ-2-HG was injected into the chiral column.

independent of one and two dimensions, respectively; after sample injection, state A was maintained for a while to remove any unnecessary compounds eluted before NBD-PZ-2-HG on the ODS column; when the NBD-PZ-2-HG peak was detected

between 28.3 and 32.3 min, the valve was switched to state B, which allowed the peak portion to flow into the sample loop. Then, the valve was switched to state A, and the NBD-PZ-2-HG solution in the sample loop was introduced into the chiral
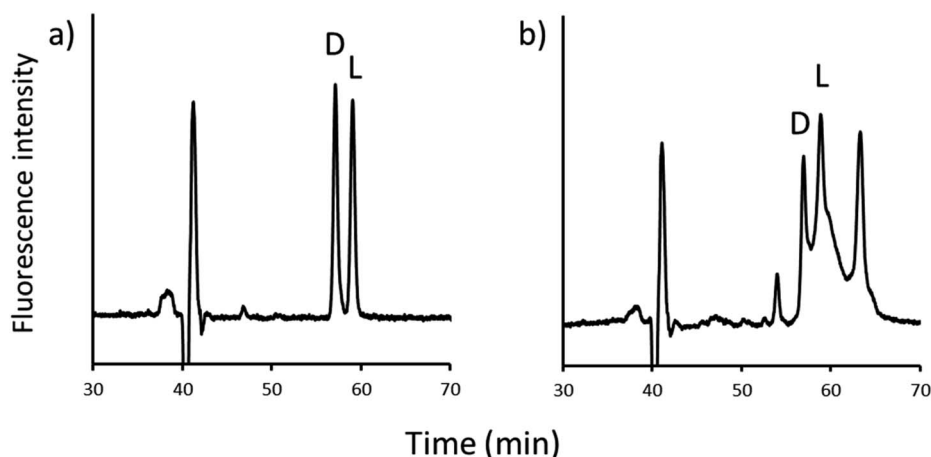
Fig. 5 Chromatograms of the second dimension in the methanol/acetonitrile/water mobile phase (80/15/5, v/v/v). (a) 2-HG sample and (b) U937 cells.
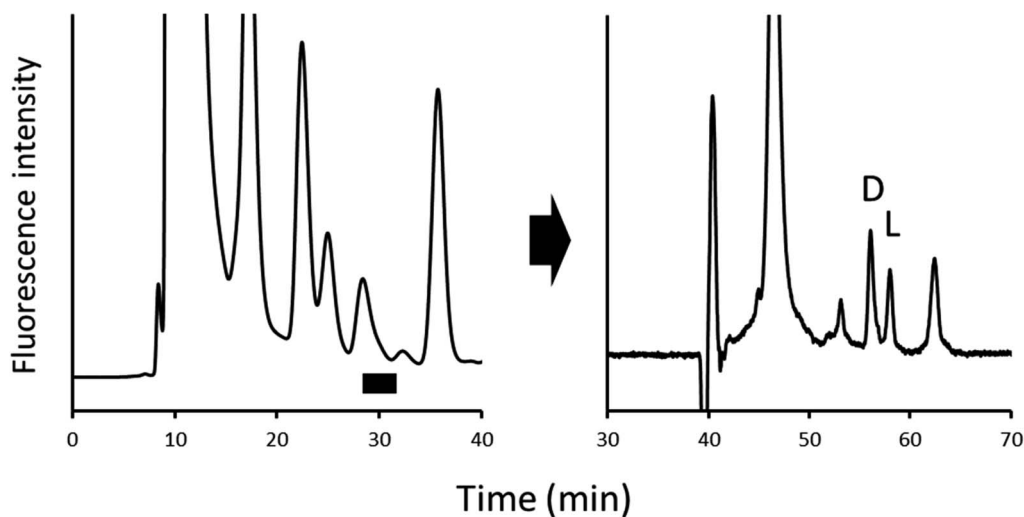
Fig. 6 Chromatograms of the first (left) and second dimensions (right) under optimized conditions.

column using pump 2. In the on-line 2D-LC method, 300 μL (a flow rate of 0.075 mL min^{-1} for 4 min) was introduced into the second dimension, while, in the previous off-line method, 750 μL (a flow rate of 0.3 mL min^{-1} for 2.5 min) was introduced.

In addition, the separation conditions for the second dimension were examined. The mobile phase of methanol/acetonitrile/water (80/15/5, v/v/v), which was optimized for off-line 2D-LC, resulted in good separation of D- and L-2-HG (resolution 2.08), as shown in Fig. 5(a). However, when the U937 cell sample was analyzed, endogenous compounds interfered with the quantification of D- and L-2-HG, as shown in Fig. 5(b). Several mobile phases were examined in this study. When formic acid aqueous solution (pH 2.0) was added, the D- and L-peaks were well separated (resolution 2.14) and quantified without any interference (Fig. 6). Accordingly, the optimized mobile phase for the second dimension was a methanol/acetonitrile/formic acid aqueous solution (pH 2.0) (80/15/5, v/v/v).

Method validation

Strong linear relationships were observed (D-2-HG: $y = 953.0x - 30.9$, $r^2 > 0.9999$, L-2-HG: $y = 875.3x - 30.0$, $r^2 > 0.9999$). The LOQs were 0.25 pmol per injection for both NBD-PZ-D-2-HG and -L-2-HG. The intra- and inter-day precisions using the standard samples are shown in Table 1.

Table 1 Intra- and inter-day precisions (RSD, %, $n = 4$)

	Intra-day				Inter-day			
	Lower LOQ	Low	Middle	High	Lower LOQ	Low	Middle	High
D-2-HG	3.50	2.73	2.38	1.04	4.69	6.21	5.53	4.49
L-2-HG	3.65	2.99	2.12	0.85	6.58	6.12	5.37	4.39

Table 2 The precision and accuracy using U937 cells

	Precision (RSD, %, $n = 4$)	Accuracy (%)			
		Lower LOQ	Low	Middle	High
D-2-HG	3.09	88.4	92.8	91.3	90.0
L-2-HG	3.18	88.2	92.7	90.9	89.7

The precision and accuracy using the U937 cells are shown in Table 2. The developed method was proven to have higher precision than the off-line 2D-LC method (intra- and inter-day precision values were less than 7.0% and 12.3%, respectively). In addition, the accuracy values were more stable than those of the off-line method (83–112%). Automatic fractionation and injection in the on-line 2D-LC method have been proven to improve the precision and stability.

Application to cell samples

The validated method was used to quantify the 2-HG enantiomers in U937 cells. The D- and L-2-HG concentrations were 13.5 ± 0.4 and 9.9 ± 0.3 pmol per 1.0 × 10^6 cells, respectively, which were in the same order of magnitude as our previous study.[21] This shows that the developed method is suitable for the analysis of intracellular 2-HG enantiomers.

Conclusions

In this study, an on-line heart-cutting 2D-LC method was developed to quantify intracellular 2-HG enantiomers. The derivatization conditions were changed to eliminate column clogging and DMTMM was used as the condensing reagent. The HPLC conditions were also optimized, and the D- and L-forms of NBD-PZ-2-HG in the cell samples were successfully separated. The precision and accuracy were better than those of the previous study owing to automatic fractionation and injection.

Using this method, the accurate quantification of 2-HG enantiomers can be realized, and the mechanism of 2-HG-related cancer should be clarified.

Author contributions

Investigation, T. O.; writing – original draft, T. O.; writing – review & editing, M. T.; supervision, M. T.

Conflicts of interest

There are no conflicts to declare.

Acknowledgements

Notes and references

1 L. W. S. Finley, *Cell*, 2023, **186**, 1670–1688.
2 L. Sun, C. Suo, S. T. Li, H. Zhang and P. Gao, *Biochim. Biophys. Acta, Rev. Cancer*, 2018, **1870**, 51–66.
3 A. Hattori, M. Tsunoda, T. Konuma, M. Kobayashi, T. Nagy, J. Glushka, F. Tayyari, D. McSkimming, N. Kannan, A. Tojo, A. S. Edison and T. Ito, *Nature*, 2017, **545**, 500–504.
4 L. Dang, D. W. White, S. Gross, B. D. Bennett, M. A. Bittinger, E. M. Driggers, V. R. Fantin, H. G. Jang, S. Jin and M. C. Keenan, *Nature*, 2009, **462**, 739–744.
5 S. Gross, R. A. Cairns, M. D. Minden, E. M. Driggers, M. A. Bittinger, H. G. Jang, M. Sasaki, S. Jin, D. P. Schenkein and S. M. Su, *J. Exp. Med.*, 2010, **207**, 339–344.
6 P. S. Ward, J. Patel, D. R. Wise, O. Abdel-Wahab, B. D. Bennett, H. A. Coller, J. R. Cross, V. R. Fantin, C. V. Hedvat and A. E. Perl, *Cancer Cell*, 2010, **17**, 225–234.
7 F. E. Bleeker, S. Lamba, S. Leenstra, D. Troost, T. Hulsebos, W. P. Vandertop, M. Frattini, F. Molinari, M. Knowles and A. Cerrato, *Hum. Mutat.*, 2009, **30**, 7–11.
8 J. Balss, J. Meyer, W. Mueller, A. Korshunov, C. Hartmann and A. von Deimling, *Acta Neuropathol.*, 2008, **116**, 597–602.
9 H. Yan, D. W. Parsons, G. Jin, R. McLendon, B. A. Rasheed, W. Yuan, I. Kos, I. Batinic-Haberle, S. Jones and G. J. Riggins, *N. Engl. J. Med.*, 2009, **360**, 765–773.
10 E. R. Mardis, L. Ding, D. J. Dooling, D. E. Larson, M. D. McLellan, K. Chen, D. C. Koboldt, R. S. Fulton, K. D. Delehaunty and S. D. McGrath, *N. Engl. J. Med.*, 2009, **361**, 1058–1066.
11 C. Hartmann, J. Meyer, J. Balss, D. Capper, W. Mueller, A. Christians, J. Felsberg, M. Wolter, C. Mawrin and W. Wick, *Acta Neuropathol.*, 2009, **118**, 469–474.
12 M. F. Amary, K. Bacsi, F. Maggiani, S. Damato, D. Halai, F. Berisha, R. Pollock, P. O'Donnell, A. Grigoriadis and T. Diss, *J. Pathol.*, 2011, **224**, 334–343.
13 J.-A. Losman and W. G. Kaelin, *Genes Dev.*, 2013, **27**, 836–852.
14 A. M. Intlekofer, R. G. Dematteo, S. Venneti, L. W. S. Finley, C. Lu, A. R. Judkins, A. S. Rustenburg, P. B. Grinaway, J. D. Chodera and J. R. Cross, *Cell Metab.*, 2015, **22**, 304–311.
15 J. F. G. Vliegenthart, J. P. Kamerling, M. Duran, G. J. Gerwig, D. Ketting, L. Bruinvis and S. K. Wadman, *J. Chromatogr.*, 1981, **222**, 276–283.
16 K. M. Gibson, H. J. Ten Brink, D. S. M. Schor, R. M. Kok, A. H. Bootsma, G. F. Hoffmann and C. Jakobs, *Pediatr. Res.*, 1993, **34**, 277–280.
17 M. S. Rashed, M. AlAmoudi and H. Y. Aboul-Enein, *Biomed. Chromatogr.*, 2000, **14**, 317–320.
18 V. Poinsignon, L. Mercier, K. Nakabayashi, M. D. David, A. Lalli, V. Penard-Lacronique, C. Quivoron, V. Saada, S. De Botton and S. Broutin, *J. Chromatogr. B Biomed. Appl.*, 2016, **1022**, 290–297.
19 Q.-Y. Cheng, J. Xiong, W. Huang, Q. Ma, W. Ci, Y.-Q. Feng and B.-F. Yuan, *Sci. Rep.*, 2015, **5**, 1–11.
20 T. Ohtawa and M. Tsunoda, *Chromatography*, 2022, **43**, 43–46.
21 T. Ohtawa, A. Hattori, M. Isokawa, M. Harada, T. Funatsu, T. Ito and M. Tsunoda, *J. Chromatogr. Open*, 2022, **1**, 100005.